



Published in final edited form as:

*Nat Neurosci.* 2015 April ; 18(4): 576–581. doi:10.1038/nn.3954.

## Frequency-specific hippocampal-prefrontal interactions during associative learning

**Scott L. Brincat and Earl K. Miller**

The Picower Institute for Learning and Memory and Department of Brain and Cognitive Sciences, Massachusetts Institute of Technology, Cambridge, MA 02139, USA

### Abstract

Much of our knowledge of the world depends on learning associations (e.g., face-name), for which the hippocampus (HPC) and prefrontal cortex (PFC) are critical. HPC-PFC interactions have rarely been studied in monkeys, whose cognitive/mnemonic abilities are akin to humans. Here, we show functional differences and frequency-specific interactions between HPC and PFC of monkeys learning object-pair associations, an animal model of human explicit memory. PFC spiking activity reflected learning in parallel with behavioral performance, while HPC neurons reflected feedback about whether trial-and-error guesses were correct or incorrect. Theta-band HPC-PFC synchrony was stronger after errors, was driven primarily by PFC to HPC directional influences, and decreased with learning. In contrast, alpha/beta-band synchrony was stronger after correct trials, was driven more by HPC, and increased with learning. Rapid object associative learning may occur in PFC, while HPC may guide neocortical plasticity by signaling success or failure via oscillatory synchrony in different frequency bands.

### Introduction

Most neurophysiological studies of PFC-HPC interactions have examined spatial memory in rodents. It seems clear, especially in primates, that the HPC and PFC have broader roles including non-spatial explicit (declarative) memory. HPC damage causes deficits in non-spatial associative learning, if implicit memory (familiarity, priming) cannot be used<sup>1–3</sup>. Likewise, PFC damage impairs explicit non-spatial associative memories, sparing implicit memory<sup>4,5</sup>. Human imaging shows activation of both areas during associative memory<sup>6,7</sup>. In rodents, there is theta synchrony between the PFC and HPC during spatial memory performance<sup>8,9</sup> and high-frequency ripple synchrony during subsequent sleep<sup>10</sup>, thought to reflect the HPC acquiring spatial information and then integrating it into cortical networks for long-term storage. A similar relationship is assumed for non-spatial memories<sup>11</sup>, but this has not been tested in primates. Here, we provide evidence that instead, in monkeys, non-spatial associations are acquired by the PFC. In contrast, HPC activity is consistent with the idea that it provides learning-related frequency-specific feedback to the PFC.

Correspondence should be addressed to E.K.M. (ekmiller@mit.edu).

**Author contributions** S.L.B. and E.K.M. designed the experiments. S.L.B. trained the monkeys, performed the experiments, and analyzed the data. S.L.B. and E.K.M. wrote the paper.

**Author information** The authors declare no competing financial interests.

## Results

### Paired associate learning task and behavioral results

We trained two adult rhesus monkeys (*Macaca mulatta*) to perform an object paired-associate learning task. The monkeys learned—through trial-and-error—four novel associations between arbitrary pairs of objects in each experimental session (Fig. 1a and b). Each of four *cue* objects (C's in Fig. 1a) was randomly paired with one of two *associate* objects ( $A_1$  or  $A_2$ ). This 4-to-2 mapping encourages prospective recall of the associate<sup>12</sup> and distinguished neural activity to the cue from retrieval of its associate. Monkeys routinely learned associations within a few hundred trials (Fig. 1c; 313 of 348 associations learned to criterion), but measures of motivation, arousal, and motor function changed little with learning (Supplementary Fig. 1). Multiple microelectrodes were lowered daily into lateral prefrontal cortex and hippocampus (Fig. 2), and each recorded spiking and LFP signals while the monkeys performed the paired-associate learning task.

### PFC and HPC neurons reflect learned associations and trial outcomes

With learning, PFC neurons increasingly showed activity after the cue that anticipated its paired associate, with an across-trial progression similar to the improvement in performance (example single neuron: Supplementary Fig. 2a and b; population summary: Fig. 3a; Spearman's  $\rho = 0.59$  with cue-epoch spike rate,  $p = 0.04$ , 2-sided permutation test). However, while HPC neuronal activity conveyed sensory signals reflecting the cue object (Supplementary Fig. 3), it did not reflect learning of the paired associate and showed no correlation with behavior ( $\rho = -0.21$ ,  $p = 0.73$ ). Instead, HPC reflected the trial outcome after the feedback (reward vs. no-reward) about whether the behavioral response was correct or incorrect. This effect was stronger in the HPC than the PFC (example single neuron: Supplementary Fig. 2c and d; population summary: Fig. 3b;  $p = 0.049$ ; 2-way area  $\times$  learning-stage permutation ANOVA), and within HPC, stronger in the output subregions (CA1, subiculum) than locally-projecting subregions (CA3, dentate gyrus;  $p = 10^{-4}$ ; Supplementary Fig. 4a). With learning, HPC activity shifted from stronger activation after incorrect to correct outcomes (Fig. 3c;  $p = 0.027$ , 2-sided permutation test on early vs. late learning stages [first vs. last third of learning trials], with number of incorrect vs. correct trials matched across learning; see Methods). This shift was present in HPC output subregions ( $p = 0.005$ ; Supplementary Fig. 4b), but not local-projection subregions ( $p = 0.83$ ; subregion  $\times$  learning-stage interaction:  $p = 0.04$ ), which may be related to a corresponding shift in communication between the HPC and PFC described below.

The learning-related change in HPC outcome bias could reflect either a sign-flip in the preference of individual neurons from incorrect to correct trials, or just a relative modulation of neurons whose outcome preference is consistent throughout learning (broadly analogous to the distinction between “global remapping” and “rate remapping” in rodent hippocampal place cells<sup>13</sup>). To distinguish between these possibilities, we trained a linear (logistic regression) classifier to discriminate correct vs. incorrect trials based on HPC activity *early* in learning, and asked whether the trained classifier weights transferred to predict trial outcome *late* in learning. The preference-flip model predicts early-learning-derived weights and late-learning activity will have largely opposing outcome preferences, and will thus

produce prediction accuracy near (or below) chance. We instead found that an early-learning trained classifier predicted the outcome on 79% of late-learning trials, comparable to 89% for a classifier both trained and tested on (distinct) late-learning trials. This provides evidence that the observed shift with learning reflects modulation of a largely invariant hippocampal neural code for trial outcome (cf. Supplementary Fig. 2d).

### Band-specific PFC-HPC synchrony reflects trial outcome and learning

We examined outcome-related neural communication using synchrony (phase-locking) between local field potentials (LFPs; Fig. 3a) recorded after the behavioral response and feedback. This revealed PFC-HPC synchrony in two frequency bands: a shorter latency theta-band (~2–6 Hz) synchrony and longer latency alpha/low-beta band (~9–16 Hz) synchrony. Alpha/beta synchrony was stronger after correct trials; theta synchrony was stronger after incorrect trials (Fig. 4a–c). Though PFC-HPC synchrony was present before the behavioral response, it did not robustly reflect trial outcome (Supplementary Fig. 5). Theta synchrony following incorrect outcomes decreased with learning (Fig. 4d and e;  $p = 10^{-4}$ ), while alpha/beta synchrony following correct outcomes increased with learning ( $p = 5 \times 10^{-4}$ , 2-sided permutation test on early vs. late learning). While the theta effect was similar across HPC subregions, the alpha/beta increase with learning only occurred for synchrony between PFC and HPC output subregions (Supplementary Fig. 6). Thus, with learning, there was a shift in PFC-HPC synchrony from theta toward higher frequencies, paralleling the shift in HPC spiking activity from incorrect to correct trials (see above).

We also examined within-area LFP phase-locking and power. While within-PFC synchrony followed a similar pattern to between-area synchrony (Supplementary Fig. 7), intra-hippocampal synchrony exhibited a distinct pattern in which theta synchrony increased—rather than decreased—with learning. This indicates the observed learning-related synchrony changes do not simply reflect state changes with global effects. LFP power, reflecting local synchrony, exhibited a pattern broadly similar to cross-area synchrony (Supplementary Fig. 8), as would be expected from an interacting system with causal links between local and long-range synchrony. Outcome selectivity in cross-area synchrony could not, however, be fully attributed to local power differences, as it remained significant even when band-specific power was balanced across correct and incorrect trials ( $P = 10^{-4}$  for both frequency bands, 1-sample bootstrap test; Supplementary Fig. 9a).

### Band-specific directionality of PFC-HPC causal influence

Theta and alpha/beta synchrony differed in the direction of putative causal influence. For theta frequencies, the phase of HPC LFPs lagged behind PFC (Fig. 5a; mean rel. phase =  $39^\circ$ ;  $p = 10^{-4}$ ; bootstrap test vs. zero phase lag), consistent with a PFC to HPC directionality; the reverse was true for alpha/beta frequencies ( $-13.5^\circ$ ;  $p = 10^{-4}$ ). We confirmed this using generalized partial directed coherence (GPDC), a frequency-domain analog of Granger causality that measures the degree to which signals can predict each other's future values. It also revealed oscillatory interactions in the theta and alpha/beta bands (Fig. 5b), with stronger theta influence (dashed lines) from PFC to HPC ( $p = 0.01$ ) and stronger alpha/beta influence (solid lines) from the HPC to PFC ( $p = 10^{-4}$ , direction factor in 2-way causal direction  $\times$  trial outcome permutation ANOVA). These differences

remained significant when band-specific LFP power was balanced across correct and incorrect trials ( $P = 10^{-4}$  for both frequency bands, direction factor in 2-way causal direction  $\times$  trial outcome permutation ANOVA); Supplementary Fig. 9b), indicating that the observed directionality cannot be explained by differences in local power. As above, theta and alpha/beta interactions were stronger for incorrect and correct trials, respectively ( $p = 10^{-4}$  for both; Fig. 5b). With learning, there were significant decreases in incorrect-reflecting PFC to HPC theta influences (Fig. 5c and d;  $p = 0.021$ ) and correct-reflecting HPC to PFC alpha/beta influences ( $p = 0.04$ , 2-sided permutation test on early vs. late learning) suggesting these interactions may be most important during the early stages of learning. In contrast, initially weak PFC to HPC alpha/beta influences reflecting correct outcomes increased with learning ( $p = 10^{-4}$ ), eventually becoming even stronger than the HPC to PFC direction ( $p = 10^{-3}$ ; interaction in 2-way causal-direction  $\times$  learning-stage permutation ANOVA).

## Discussion

These results suggest different roles and interactions between the PFC and HPC during object associative learning. Only PFC neurons showed neural correlates of learning the paired associates. The HPC was more engaged when feedback was given about whether the trial was correct or incorrect. Early in learning, incorrect outcomes activated HPC neurons and promoted cross-area theta synchrony with a stronger influence from the PFC to the HPC. Correct outcomes, in contrast, promoted alpha/beta-band synchrony that was initially stronger in the HPC to PFC direction. But as learning progressed, correct outcomes increasingly evoked PFC to HPC alpha/beta-band influences and HPC neuronal spiking. This shift in HPC outcome coding (and other properties; Supplementary Fig. 10) distinguishes it from unipolar positive and negative reward-prediction-error signals in the midbrain dopaminergic nuclei<sup>14</sup> and lateral habenula<sup>15</sup>, respectively. It may, however, reflect a functional shift in the importance of negative and positive feedback. Early in trial-and-error learning, errors provide critical information about which pairs of objects should *not* be associated. But once associations are learned, errors are more likely to simply reflect lapses in response inhibition or attention rather than true errors of associative choice. In contrast, positive feedback following correct trials<sup>16</sup>, and the likely resulting dopamine release in hippocampus<sup>17</sup>, have been shown to preferentially enhance long-term consolidation of new learning. Thus, the shift in HPC bias from incorrect to correct outcomes as learning progresses is consistent with a transition from neural signals that support acquisition to those that promote consolidation.

The HPC is critical for formation of explicit memories. Rodent neurophysiological studies suggest it acquires spatial memories and consolidates them in the neocortex, including PFC<sup>8,10</sup>. The primate HPC shows rapid activity changes related to spatial associative learning<sup>18</sup>. But the HPC is also known to be critical for non-spatial memory in rodents<sup>11,19</sup> and especially in primates, where it plays a general role in explicit memory formation<sup>1,3</sup>. Lesion studies have suggested that perirhinal cortex—part of the medial temporal lobe system<sup>3</sup> that includes the HPC—may be more critical for object associative learning than the HPC<sup>19,20</sup>, and neural correlates of object associations have been seen in perirhinal, prefrontal, and inferotemporal cortex<sup>12,21–23</sup>. However, these studies examined associations that were familiar or learned gradually (over days or weeks), situations known to favor

neocortical representation. Our results suggest that rapid acquisition of object associations also occurs in the neocortex, not the HPC, perhaps particularly the PFC given its importance for behavioral flexibility. Object associations may lack the context required for explicit HPC representation<sup>24</sup>.

Both the HPC and PFC signal trial outcome, differentiating between correct and error trials<sup>25,26</sup>. Our results suggest this information is communicated between HPC and PFC via synchrony at different frequencies: theta for incorrect and alpha/beta for correct. Human and animal studies suggest that oscillatory activity is associated with memory encoding and retrieval<sup>27–29</sup>, as well as other cognitive processes<sup>30–32</sup>. Higher frequency (gamma) oscillations are thought to underlie the transient formation of local neuronal ensembles, while lower frequencies may recruit larger networks due to their longer integration times<sup>31,33,34</sup>. Thus, the lower frequency (theta and alpha/beta) synchrony we observed may reflect formation of larger networks connecting PFC, HPC, and likely many other cortical and subcortical structures. Further experimentation will be necessary to delineate the extent of these networks and dissect out how each of their nodes function in learning. Human EEG also shows theta oscillations with a frontal source reflecting conflict or error<sup>35</sup>; our results suggest these oscillations are propagated to hippocampus during learning. We did not, however, observe the sustained bouts of theta oscillations typically seen in locomoting rodents<sup>8,9,36</sup>; it remains an open question whether our theta-band synchrony reflects a distinct or related phenomenon.

But what computational role might these particular frequencies have? Growing evidence suggests beta oscillations are ideal for maintaining active cell assemblies and their associated cognitive states<sup>37</sup>. This hypothesis is consistent with the idea that alpha/beta oscillations might have a role in maintaining neural representations active during correct associations. Studies of synaptic plasticity have also shown that low-frequency synaptic stimulation fosters long-term depression, while high-frequency stimulation fosters long-term potentiation<sup>38</sup>, with the crossover point at ~8–10 Hz. PFC-HPC theta interactions may therefore have weakened synapses active during incorrect associations, while alpha/beta interactions strengthened those active for the correct associations.

In sum, these observations show that rapid formation of non-spatial associations may occur within the PFC, not the HPC. The main role of the HPC appears to be signalling trial outcome, signals which are communicated with PFC via band-specific oscillatory synchrony and may be involved in guiding neocortical learning. The results also provide further support for the idea that synchrony in different frequency bands may have functionally different roles in neural communication<sup>30,34</sup>.

**Methods** and any associated references are available in the Supplementary Materials.

## Supplementary Material

Refer to Web version on PubMed Central for supplementary material.

## Acknowledgments

This work was supported by NIMH Conte Center grant P50-MH094263-03 (E.K.M.), NIMH fellowship F32-MH081507 (S.L.B.), and The Picower Foundation. We thank E. Antzoulatos, A. Bastos, J. Donoghue, N. Kopell, S. Kornblith, R. Loonis, M. Lundqvist, M. Moazami, V. Puig, J. Rose, J. Roy, A. Salazar-Gómez, L. Tran, and M. Wilson for helpful comments and suggestions, and D. Altschul, B. Gray, M. Histed, D. Ouellette, and the MIT veterinary staff for technical assistance.

## References

1. Scoville WB, Milner B. Loss Of Recent Memory After Bilateral Hippocampal Lesions. *J Neurol Neurosurg Psychiatry*. 1957; 20:11–21. [PubMed: 13406589]
2. Cohen NJ, Squire LR. Preserved Learning and Retention of Pattern-Analyzing Skill in Amnesia: Dissociation of Knowing How and Knowing That. *Science*. 1980; 210:207–210. [PubMed: 7414331]
3. Squire LR, Stark CEL, Clark RE. The medial temporal lobe. *Annu Rev Neurosci*. 2004; 27:279–306. [PubMed: 15217334]
4. Gutnikov SA, Ma YY, Gaffan D. Temporo-frontal Disconnection Impairs Visual-visual Paired Association Learning but not Configural Learning in Macaca Monkeys. *Eur J Neurosci*. 1997; 9:1524–1529. [PubMed: 9240410]
5. Farovik A, Dupont LM, Arce M, Eichenbaum H. Medial Prefrontal Cortex Supports Recollection, But Not Familiarity, in the Rat. *J Neurosci*. 2008; 28:13428–13434. [PubMed: 19074016]
6. Sperling RA, et al. Encoding novel face-name associations: A functional MRI study. *Hum Brain Mapp*. 2001; 14:129–139. [PubMed: 11559958]
7. Kim H. Neural activity that predicts subsequent memory and forgetting: A meta-analysis of 74 fMRI studies. *NeuroImage*. 2011; 54:2446–2461. [PubMed: 20869446]
8. Jones MW, Wilson MA. Theta Rhythms Coordinate Hippocampal–Prefrontal Interactions in a Spatial Memory Task. *PLoS Biol*. 2005; 3:e402. [PubMed: 16279838]
9. Hyman JM, Zilli EA, Paley AM, Hasselmo ME. Medial prefrontal cortex cells show dynamic modulation with the hippocampal theta rhythm dependent on behavior. *Hippocampus*. 2005; 15:739–749. [PubMed: 16015622]
10. Siapas AG, Wilson MA. Coordinated interactions between hippocampal ripples and cortical spindles during slow-wave sleep. *Neuron*. 1998; 21:1123–1128. [PubMed: 9856467]
11. Eichenbaum H, Dudchenko P, Wood E, Shapiro M, Tanila H. The hippocampus, memory, and place cells: Is it spatial memory or a memory space? *Neuron*. 1999; 23:209–226. [PubMed: 10399928]
12. Rainer G, Rao SC, Miller EK. Prospective coding for objects in primate prefrontal cortex. *J Neurosci*. 1999; 19:5493–5505. [PubMed: 10377358]
13. Colgin LL, Moser EI, Moser MB. Understanding memory through hippocampal remapping. *Trends Neurosci*. 2008; 31:469–477. [PubMed: 18687478]
14. Schultz W. Predictive reward signal of dopamine neurons. *J Neurophysiol*. 1998; 80:1–27. [PubMed: 9658025]
15. Matsumoto M, Hikosaka O. Lateral habenula as a source of negative reward signals in dopamine neurons. *Nature*. 2007; 447:1111–1115. [PubMed: 17522629]
16. Abe M, et al. Reward Improves Long-Term Retention of a Motor Memory through Induction of Offline Memory Gains. *Curr Biol*. 2011; 21:557–562. [PubMed: 21419628]
17. Bethus I, Tse D, Morris RGM. Dopamine and Memory: Modulation of the Persistence of Memory for Novel Hippocampal NMDA Receptor-Dependent Paired Associates. *J Neurosci*. 2010; 30:1610–1618. [PubMed: 20130171]
18. Wirth S, et al. Single neurons in the monkey hippocampus and learning of new associations. *Science*. 2003; 300:1578–1581. [PubMed: 12791995]
19. Bunsey M, Eichenbaum H. Conservation of memory function in rats and humans. *Nature*. 1996; 379:255–257. [PubMed: 8538790]

20. Murray EA, Gaffan D, Mishkin M. Neural substrates of visual stimulus-stimulus association in rhesus monkeys. *J Neurosci.* 1993; 13:4549–4561. [PubMed: 8410203]
21. Sakai K, Miyashita Y. Neural organization for the long-term memory of paired associates. *Nature.* 1991; 354:152–155. [PubMed: 1944594]
22. Erickson CA, Desimone R. Responses of macaque perirhinal neurons during and after visual stimulus association learning. *J Neurosci.* 1999; 19:10404–10416. [PubMed: 10575038]
23. Messinger A, Squire LR, Zola SM, Albright TD. Neuronal representations of stimulus associations develop in the temporal lobe during learning. *Proc Natl Acad Sci.* 2001; 98:12239–12244. [PubMed: 11572946]
24. Eichenbaum H, Sauvage M, Fortin N, Komorowski R, Lipton P. Towards a functional organization of episodic memory in the medial temporal lobe. *Neurosci Biobehav Rev.* 2012; 36:1597–1608. [PubMed: 21810443]
25. Wirth S, et al. Trial Outcome and Associative Learning Signals in the Monkey Hippocampus. *Neuron.* 2009; 61:930–940. [PubMed: 19324001]
26. Histed MH, Pasupathy A, Miller EK. Learning Substrates in the Primate Prefrontal Cortex and Striatum: Sustained Activity Related to Successful Actions. *Neuron.* 2009; 63:244–253. [PubMed: 19640482]
27. Jutras MJ, Fries P, Buffalo EA. Gamma-Band Synchronization in the Macaque Hippocampus and Memory Formation. *J Neurosci.* 2009; 29:12521–12531. [PubMed: 19812327]
28. Düzel E, Penny WD, Burgess N. Brain oscillations and memory. *Curr Opin Neurobiol.* 2010; 20:143–149. [PubMed: 20181475]
29. Fell J, Axmacher N. The role of phase synchronization in memory processes. *Nat Rev Neurosci.* 2011; 12:105–118. [PubMed: 21248789]
30. Fries P. A mechanism for cognitive dynamics: neuronal communication through neuronal coherence. *Trends Cogn Sci.* 2005; 9:474–480. [PubMed: 16150631]
31. Buschman TJ, Miller EK. Top-Down Versus Bottom-Up Control of Attention in the Prefrontal and Posterior Parietal Cortices. *Science.* 2007; 315:1860–1862. [PubMed: 17395832]
32. Siegel M, Warden MR, Miller EK. Phase-dependent neuronal coding of objects in short-term memory. *Proc Natl Acad Sci.* 2009; 106:21341–21346. [PubMed: 19926847]
33. Kopell N, Ermentrout GB, Whittington MA, Traub RD. Gamma rhythms and beta rhythms have different synchronization properties. *Proc Natl Acad Sci.* 2000; 97:1867–1872. [PubMed: 10677548]
34. Buzsáki G, Draguhn A. Neuronal Oscillations in Cortical Networks. *Science.* 2004; 304:1926–1929. [PubMed: 15218136]
35. Luu P, Tucker DM, Makeig S. Frontal midline theta and the error-related negativity: neurophysiological mechanisms of action regulation. *Clin Neurophysiol.* 2004; 115:1821–1835. [PubMed: 15261861]
36. Buzsáki G, Moser EI. Memory, navigation and theta rhythm in the hippocampal-entorhinal system. *Nat Neurosci.* 2013; 16:130–138. [PubMed: 23354386]
37. Engel AK, Fries P. Beta-band oscillations—signalling the status quo? *Curr Opin Neurobiol.* 2010; 20:156–165. [PubMed: 20359884]
38. Dudek SM, Bear MF. Homosynaptic long-term depression in area CA1 of hippocampus and effects of N-methyl-D-aspartate receptor blockade. *Proc Natl Acad Sci.* 1992; 89:4363–4367. [PubMed: 1350090]
39. Skaggs WE, et al. EEG Sharp Waves and Sparse Ensemble Unit Activity in the Macaque Hippocampus. *J Neurophysiol.* 2007; 98:898–910. [PubMed: 17522177]
40. Nelson MJ, Pouget P, Nilsen EA, Patten CD, Schall JD. Review of signal distortion through metal microelectrode recording circuits and filters. *J Neurosci Methods.* 2008; 169:141–157. [PubMed: 18242715]
41. Miller EK, Gochin PM, Gross CG. Habituation-like decrease in the responses of neurons in inferior temporal cortex of the macaque. *Vis Neurosci.* 1991; 7:357–362. [PubMed: 1751421]
42. Xiang JZ, Brown MW. Neuronal responses related to long-term recognition memory processes in prefrontal cortex. *Neuron.* 2004; 42:817–829. [PubMed: 15182720]

43. Yanike M, Wirth S, Smith AC, Brown EN, Suzuki WA. Comparison of Associative Learning-Related Signals in the Macaque Perirhinal Cortex and Hippocampus. *Cereb Cortex*. 2009; 19:1064–1078. [PubMed: 18936274]
44. Manly, BFJ. Randomization, bootstrap, and Monte Carlo methods in biology. Chapman & Hall/CRC; 2007.
45. Torrence C, Compo G. A practical guide to wavelet analysis. *Bull Am Meteorol Soc*. 1998; 79:61–78.
46. Cui J, Xu L, Bressler SL, Ding M, Liang H. BSMART: A Matlab/C toolbox for analysis of multichannel neural time series. *Neural Netw*. 2008; 21:1094–1104. [PubMed: 18599267]
47. Oostenveld R, Fries P, Maris E, Schoffelen JM. FieldTrip: Open Source Software for Advanced Analysis of MEG, EEG, and Invasive Electrophysiological Data. *Comput Intell Neurosci*. 2011; 2011:1–9. [PubMed: 21837235]
48. Bokil H, Andrews P, Kulkarni JE, Mehta S, Mitra PP. Chronux: A platform for analyzing neural signals. *J Neurosci Methods*. 2010; 192:146–151. [PubMed: 20637804]
49. Gallistel CR, Fairhurst S, Balsam P. The learning curve: Implications of a quantitative analysis. *Proc Natl Acad Sci U S A*. 2004; 101:13124–13131. [PubMed: 15331782]
50. Zar, JH. Biostatistical analysis. Prentice-Hall/Pearson; 2010.
51. Olejnik S, Algina J. Generalized Eta and Omega Squared Statistics: Measures of Effect Size for Some Common Research Designs. *Psychol Methods*. 2003; 8:434–447. [PubMed: 14664681]
52. Meyers, EM.; Kreiman, G. Visual Population Codes. MIT Press; 2012. p. 517-538.
53. Kalcher J, Pfurtscheller G. Discrimination between phase-locked and non-phase-locked event-related EEG activity. *Electroencephalogr Clin Neurophysiol*. 1995; 94:381–384. [PubMed: 7774524]
54. Ding M, Bressler SL, Yang W, Liang H. Short-window spectral analysis of cortical event-related potentials by adaptive multivariate autoregressive modeling: data preprocessing, model validation, and variability assessment. *Biol Cybern*. 2000; 83:35–45. [PubMed: 10933236]
55. Lachaux JP, Rodriguez E, Martinerie J, Varela FJ. Measuring phase synchrony in brain signals. *Hum Brain Mapp*. 1999; 8:194–208. [PubMed: 10619414]
56. Vinck M, van Wingerden M, Womelsdorf T, Fries P, Pennartz CMA. The pairwise phase consistency: A bias-free measure of rhythmic neuronal synchronization. *NeuroImage*. 2010; 51:112–122. [PubMed: 20114076]
57. Fisher, NI. Statistical analysis of circular data. Univ. Press; 1995.
58. Baccalá, LA.; Sameshima, K.; Takahashi, DY. Generalized partial directed coherence; Digital Signal Processing, 2007 15th International Conference on; 2007. p. 163-166.
59. Granger CW. Investigating causal relations by econometric models and cross-spectral methods. *Econ J Econ Soc*. 1969:424–438.
60. Morf M, Vieira A, Lee DT, Kailath T. Recursive multichannel maximum entropy spectral estimation. *Geosci Electron IEEE Trans*. 1978; 16:85–94.
61. Geweke J. Measurement of linear dependence and feedback between multiple time series. *J Am Stat Assoc*. 1982; 77:304–313.
62. Hess Eckhard H, Polt James M. Pupil size as related to interest value of visual stimuli. *Science*. 1960; 132:349–350. [PubMed: 14401489]
63. Kennerley SW, Wallis JD. Reward-Dependent Modulation of Working Memory in Lateral Prefrontal Cortex. *J Neurosci*. 2009; 29:3259–3270. [PubMed: 19279263]
64. Nassar MR, et al. Rational regulation of learning dynamics by pupil-linked arousal systems. *Nat Neurosci*. 2012; 15:1040–1046. [PubMed: 22660479]
65. Shepherd SV, Lanzilotto M, Ghazanfar AA. Facial Muscle Coordination in Monkeys during Rhythmic Facial Expressions and Ingestive Movements. *J Neurosci*. 2012; 32:6105–6116. [PubMed: 22553017]
66. Funahashi S, Bruce CJ, Goldman-Rakic PS, et al. Mnemonic coding of visual space in the monkey's dorsolateral prefrontal cortex. *J Neurophysiol*. 1989; 61:331–349. [PubMed: 2918358]
67. Cromer JA, Machon M, Miller EK. Rapid association learning in the primate prefrontal cortex in the absence of behavioral reversals. *J Cogn Neurosci*. 2011; 23:1823–1828. [PubMed: 20666598]



68. Merletti R, Di Torino P. Standards for reporting EMG data. *J Electromyogr Kinesiol.* 1999; 9:3–4.
69. Schoffelen JM. Neuronal Coherence as a Mechanism of Effective Corticospinal Interaction. *Science.* 2005; 308:111–113. [PubMed: 15802603]

Author Manuscript

Author Manuscript

Author Manuscript

Author Manuscript

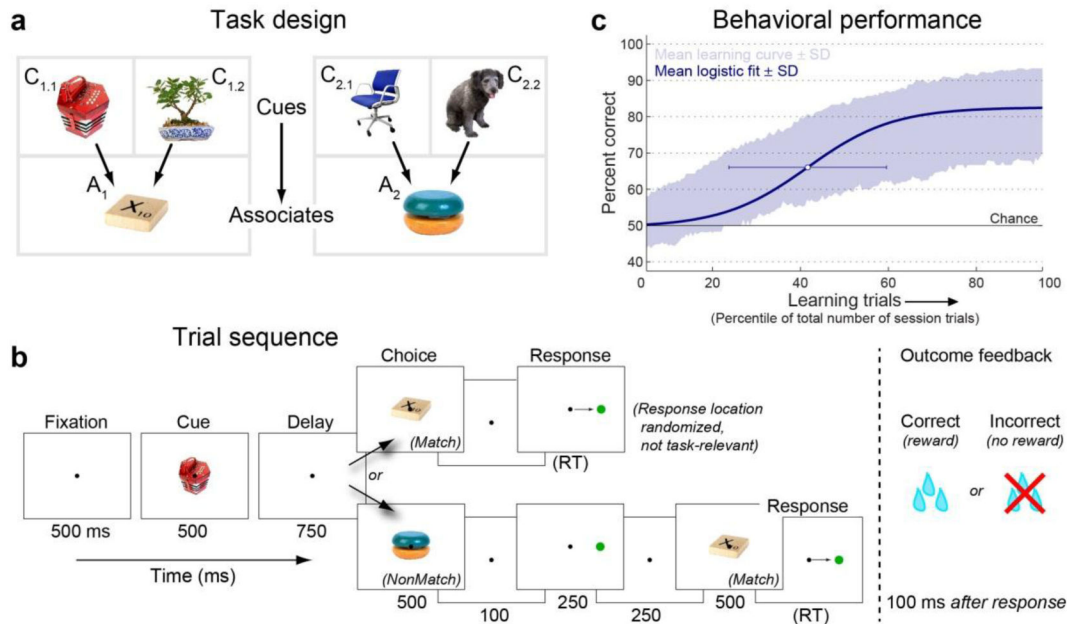


**Figure 1. Paired-associate learning task**

(a) Task design. Each session, four objects were designated as *cue* objects; each was arbitrarily paired with one of two *associate* objects. (b) Task trial sequence. After central fixation, a cue object was followed by a short delay and a choice object. If it was that cue's paired associate, monkeys had to saccade to a target (whose varied location was not task-relevant); otherwise, they were required to withhold response through another delay until the correct associate was presented. Correct choices were rewarded with juice; incorrect choices resulted in no reward and were signaled by a red error screen and 3-second "time-out". Task period durations given in ms below panels (RT: reaction time). (c) Learning performance. Shaded area: mean  $\pm$  SD of percent correct performance across all 348 associations (87 sessions), plotted as a function of the percentile of each session's trials (mean  $\pm$  SD trials per session:  $1117 \pm 125$ ). Blue curve: average sigmoidal learning curve fit to each association. White dot: mean  $\pm$  SD of fit curve centers.

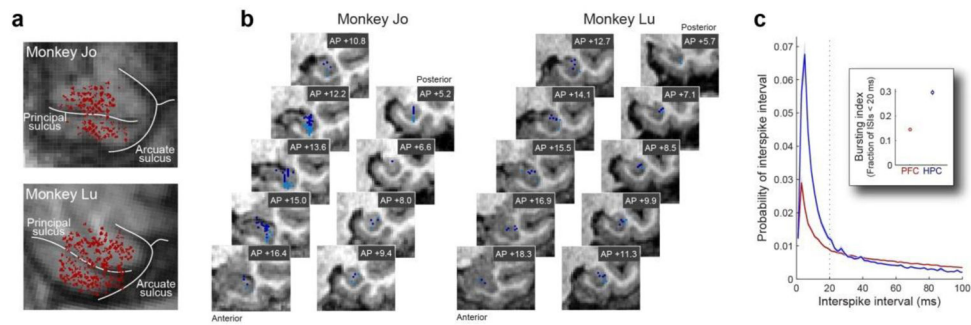


**Figure 2. Prefrontal and hippocampal recording locations**

(a) Prefrontal recording sites in two monkeys, “Jo” and “Lu”, projected onto a tangential MRI slice. Each dot represents a location where neurons were recorded. Recordings spanned a broad region of dorsolateral and ventrolateral PFC (including parts of areas 46, 45, and 8). (b) Hippocampal recording sites, plotted on an anterior-to-posterior series of coronal MRI slices (labeled with mm relative to interaural line along the anterior-posterior axis). Dark blue: locally-projecting subregions (dentate gyrus, CA3, CA2). Light blue: output subregions (CA1, subiculum). Recordings spanned all subregions of the anterior ~3/4 of the hippocampal formation. (c) Hippocampal neurons exhibit characteristic bursty firing. Population mean ( $\pm$  SEM) interspike interval (ISI) histograms showing the probability of each ISI averaged across all PFC (red) and HPC (blue) putative principal neurons (putative fast-spiking interneurons were discriminated based on spike waveform and firing rate and excluded from this plot). Inset: population mean ( $\pm$  SEM) spike bursting index<sup>39</sup>—the fraction of each neuron’s ISIs < 20 ms. Both plots illustrate the distinctive burstiness of hippocampal neurons in comparison to neocortical neurons.

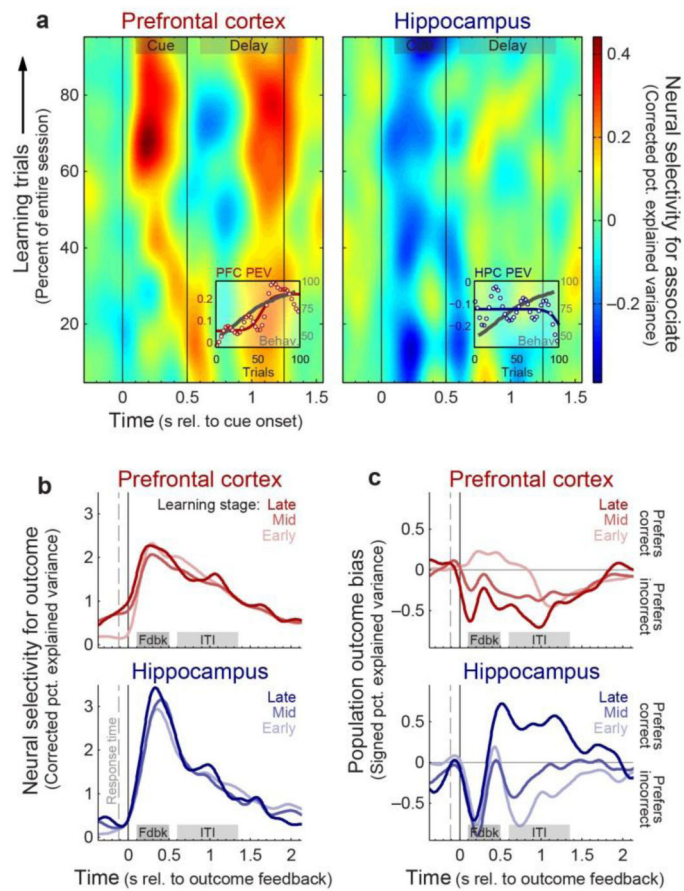


**Figure 3. Prefrontal neurons reflect learned associations; hippocampal neurons reflect trial outcome**

(a) Mean percent of variance explained (PEV) by learned associate objects in PFC (left;  $n = 319$  neurons) and HPC (right;  $n = 199$ ) spiking activity, plotted across time after cue onset and learning trials. Bias correction results in negative values for some trials/times where values are less than expected based on selectivity for random combinations of cue objects (see Methods). Gray bars: analytical epochs focusing on cue and delay periods. Insets: behavioral (gray) and neural “learning curves”—mean cue-epoch PEV across trials. Only PFC shows learning of associates in parallel with behavior. (b) Mean percent of variance in PFC (top) and HPC (bottom) neurons explained by trial outcome (correct vs. incorrect), plotted across time after outcome feedback (reward vs. no-reward) for early, middle, and late learning stages (light-to-dark colors). Gray bars: analytical epochs focusing on transient responses to outcome feedback and sustained activity during the inter-trial interval (ITI). Outcome is represented more strongly in HPC in the outcome feedback epoch. (c) Mean bias (signed PEV; see Methods) in PFC (top) and HPC (bottom) neurons for correct (positive values) vs. incorrect (negative) outcomes, as a function of time and learning stages. HPC shifts from incorrect to correct outcomes with learning. Though there is a significant area  $\times$  learning-stage interaction ( $p = 0.03$ ), PFC shows no significant change with learning ( $p = 0.3$ ).

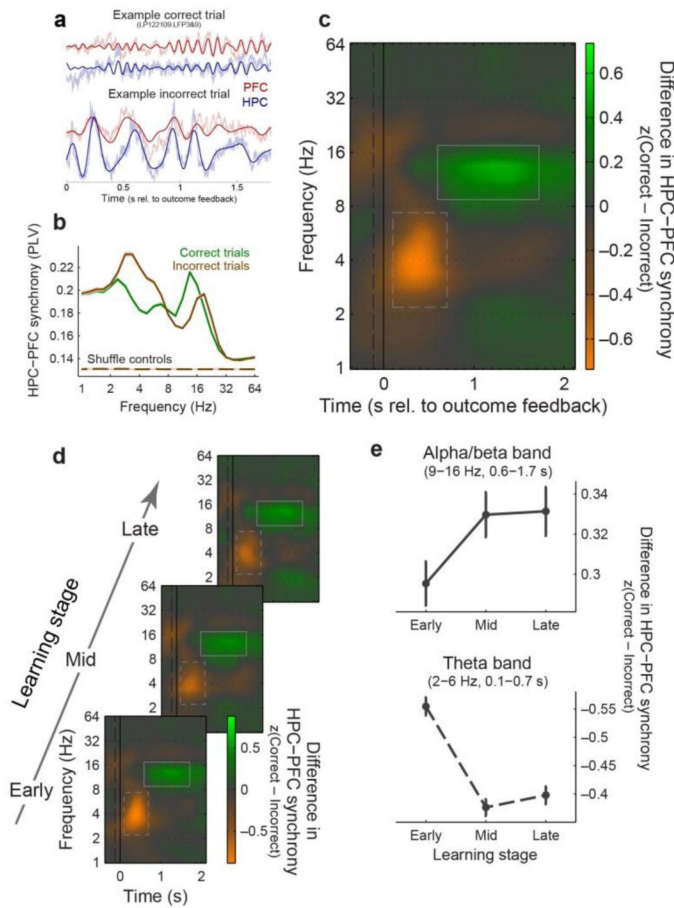


**Figure 4. Hippocampal-prefrontal oscillatory synchrony carries learning-related information about trial outcome**

(a) Example LFPs from a pair of sites in HPC (blue) and PFC (red) following a correct (top) and an incorrect (bottom) trial. Lighter colors: raw LFPs; darker colors: LFPs filtered within the 9–16 Hz (top) and 2–6 Hz (bottom) bands. (b) Mean synchrony ( $\pm$  SEM) between HPC and PFC LFPs, plotted as a function of frequency, following correct (green) and incorrect (brown) outcomes. Synchrony is computed as the across-trial phase-locking value (PLV), calculated within the feedback and ITI epochs (100–1725 ms after outcome feedback), and is averaged across all 970 electrode pairs and sessions. Dashed curves: mean synchrony ( $\pm$  SEM) expected by chance (based on shuffling HPC and PFC signals across trials), which is nearly identical across trial outcome and frequency. (c) Mean z-scored difference in HPC-PFC synchrony (dPLV) between correct and incorrect trials, plotted as spectrograms across time and frequency. Theta-band (dashed rectangle) and alpha/beta-band (solid rectangle) synchrony were stronger for incorrect and correct outcomes, respectively. (d) Mean dPLV as a function of learning (bottom to top: early, middle, and late learning stages). (e) Summary of synchrony learning effects—mean dPLV ( $\pm$  SEM) pooled within the alpha/beta-band (top) and theta-band (bottom; note that higher values in this plot reflect stronger *negative* PLV differences) regions of interest, as a function of learning stage. Theta (incorrect) synchrony decreases with learning, while alpha/beta (correct) increases.

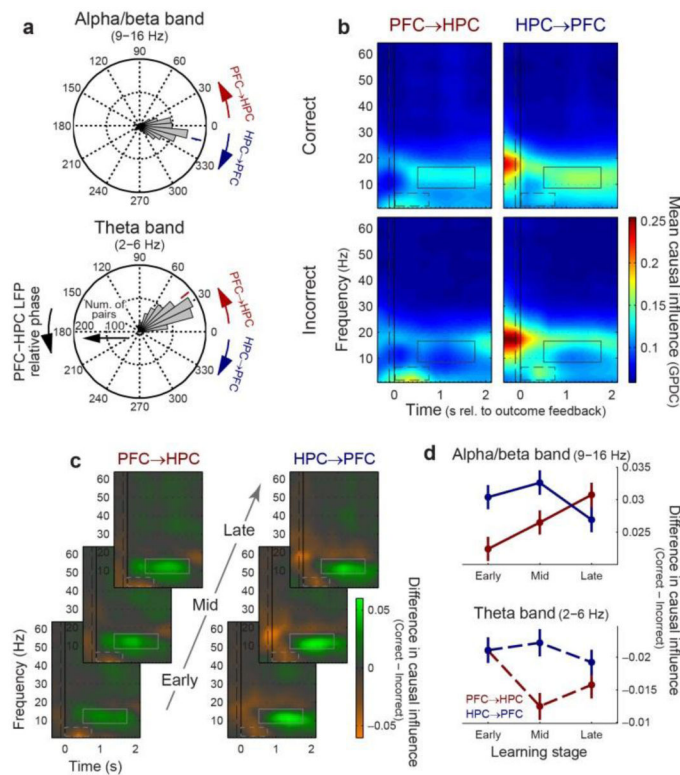


**Figure 5. Stronger theta PFC→HPC directional influence; stronger HPC→PFC alpha/beta influence**

(a) Angular histograms of mean PFC-HPC LFP phase lag ( $n = 970$  electrode pairs), pooled within alpha/beta-band (top) and theta-band (bottom) regions of interest. Colored tick marks indicate mean across all pairs. HPC leads for alpha/beta frequencies, while PFC leads for theta. (b) Frequency-domain directional influences (generalized partial directed coherence; GPDC) from PFC to HPC (left;  $n = 970$  electrode pairs) and from HPC to PFC (right;  $n = 970$ ), following correct (top) and incorrect (bottom) trials. GPDC is plotted as spectrograms across time and frequency. Overall, alpha/beta-band influences (solid rectangles) are stronger from HPC to PFC and for correct, while theta-band influences (dashed rectangles) are stronger from PFC to HPC and for incorrect trials. (c) Cross-area directional influences across learning. Selectivity for trial outcome is quantified by the difference in directional strength (GPDC) between correct and incorrect outcomes, and is plotted separately for each direction (PFC→HPC, left; HPC→PFC, right) and learning stage (bottom to top). (d) Summary of learning effects: mean difference (correct – incorrect) in causal influence ( $\pm$  s.e.m.) pooled in the alpha/beta-band (top) and theta-band (bottom) regions of interest, as a function of learning stage. With learning, theta interactions showed a decreasing trend, whereas alpha/beta interactions shifted from a HPC→PFC to PFC→HPC directionality.